agronomy

MDPI

Article

Motion Control Design and Parameter Optimization of an Alternating Seedling Picking and Dropping System for a Two-Row Automatic Transplanter

Jingyi Sun, Jianping Hu *, Xinxin Chen, Wei Liu, Qingxiang Yang, Zhongpeng Zhang and Haoran Wu

School of Agricultural Equipment Engineering, Jiangsu University, Zhenjiang 212013, China; 2212416020@stmail.ujs.edu.cn (J.S.); xxchen@ujs.edu.cn (X.C.); mario_liu@ujs.edu.cn (W.L.); 2222516065@stmail.ujs.edu.cn (Q.Y.); 2222516071@stmail.ujs.edu.cn (Z.Z.); 2222516054@stmail.ujs.edu.cn (H.W.)
* Correspondence: hujp@ujs.edu.cn

Abstract

To address the numerous operational steps and structural complexity associated with existing two-row automatic transplanters that use stepwise tray conveying, whole-row seedling picking with multiple claws, and rotary seedling distribution, an alternating seedling picking and dropping system was developed. The system combines trays that remain stationary during picking, left and right claw groups that alternately pick and drop seedlings, and a fixed seedling distribution device that alternately feeds seedlings to the planting units. The seedling trays are mounted on a two-station rotary platform and remain stationary during picking. Linear motion modules drive two groups of picking claws, each consisting of two claws, in the longitudinal and transverse directions to pick and drop seedlings. Two groups of fixed seedling distribution tubes receive the seedlings and sequentially feed them to the duckbill planting units. To achieve precise and efficient seedling picking, a picking path was planned based on the tray cell arrangement, and an S-curve acceleration and deceleration strategy was applied to determine motion timing parameters for different seedling positions. Based on the receiving window of the planting mechanism, spatial and temporal matching relationships were established among the seedling picking, dropping, and planting processes. The continuous operating sequence for an entire tray was calculated to determine the operating parameters and time margins at each picking position. Experiments and parameter optimization were conducted to investigate the effects of the distribution tube opening instant, planting frequency, and seedling receiving height on seedling receiving deviation. The selected operating parameters were a distribution tube opening instant of 0.56 s, a planting frequency of 51 seedlings per row per minute, and a seedling receiving height of approximately 49 mm. Separate machine tests yielded a picking and dropping success rate of 96.48% and a receiving success rate of 100% under the selected operating conditions. These results support the feasibility of the proposed system under the conditions evaluated.

Keywords: seedling picking and dropping system; motion control; timing coordination; parameter optimization

Check for updates

Academic Editor: Marco Fontanelli

Received: 8 October 2026
Revised: 27 October 2026
Accepted: 1 November 2026
Published: 4 November 2026

Copyright: © 2026 by the authors. Licensee MDPI, Basel, Switzerland. This article is an open access article distributed under the terms and conditions of the Creative Commons Attribution (CC BY) license.

1. Introduction

China is the world's largest producer of greenhouse vegetables. Mechanical transplanting of vegetable seedlings offers high productivity, precise operation, and consistent

planting quality. With the expansion of protected vegetable cultivation and the growing demand for continuous transplanting, equipment for transplanting vegetable plug seedlings is increasingly being developed for higher operating speeds, greater automation, and improved precision [1–5]. Vegetables such as cabbage and solanaceous crops are commonly planted in two rows per bed, placing greater demands on continuous seedling supply, coordinated picking and dropping, and reliable seedling receiving [6–9]. As the primary carriers of plug seedlings during transplanting, seedling trays directly influence the seedling supply method, picking path, and operating cycle through their dimensions and cell arrangement [10–12]. Plug seedlings are small, their growing substrate is prone to disintegration, and their orientation can readily change [13,14]. These characteristics impose stringent requirements on mechanical transplanting: coordinated operation must be maintained while minimizing damage to seedlings and their substrate during picking, dropping, feeding, and receiving, and ensuring the stability of each stage during continuous operation [15–19]. Therefore, developing a seedling picking and dropping system with a simple structure, reliable functionality, and coordinated continuous operation is essential to improving the continuity and reliability of automatic transplanting of vegetable plug seedlings [20–22].

To meet the demand for automated vegetable transplanting, researchers worldwide have extensively investigated the key stages of seedling picking and dropping systems. Yao et al. [23] developed a system based on coordinated multi-sensor operation, combining transverse tray advancement with the longitudinal movement of the picking device to achieve continuous seedling picking. The picking device consisted of two claw assemblies with six picking claws in total. Three adjacent seedlings were picked simultaneously on one side, and the next picking operation was performed after advancing by a prescribed longitudinal interval. The extracted plug seedlings were distributed through fixed seedling distribution tubes.

Jin et al. [24] developed an automatic vegetable plug seedling transplanting device in which a lead-screw-driven linear stage and a dual-chain mechanism provided transverse and longitudinal tray movement, respectively. Seedling picking was achieved by coordinating tray movement with a rotary picking mechanism. A single picking claw gripped the plug seedlings individually, and the tray was advanced to the next row after all seedlings in the current row had been picked. The extracted seedlings were dropped directly into the planting mechanism without a separate seedling distribution device.

Han et al. [25] developed a seedling picking and dropping system equipped with a flexible plug seedling gripper with a wide opening. A dual-chain conveyor transported the trays transversely into the gripper's working area. The picking device comprised two symmetrically arranged pneumatic fingers that gripped and extracted one plug seedling at a time. The manipulator transferred the extracted seedlings directly to the target position without a separate seedling distribution mechanism.

Ma et al. [26] developed a pneumatic whole-row seedling picking system for automatic vegetable transplanters. The system combined transverse tray conveying with pivoting picking claws to achieve continuous picking. Six or eight picking claws were arranged side by side to extract an entire row of seedlings simultaneously. After extraction, the plug seedlings were sequentially dropped into continuously moving seedling distribution cups.

The seedling picking and dropping system of the Ferrari FPA2 single-disk vegetable transplanter [27] employed a horizontal tray conveyor for stepwise transverse tray advancement. The picking device consisted of two rows of four claws each. A horizontal drive unit and an electric linear actuator produced reciprocating linear motion, allowing eight plug seedlings to be picked simultaneously in a single operation. Seedlings were distributed using a single rotary disk. After picking, the seedlings were guided into openings arranged

along the inner and outer rings of the disk and carried to the dropping position as the disk rotated, before being planted.

Li et al. [28] developed a seedling picking and dropping system with a following motion, in which a pneumatic cylinder and a ratchet mechanism drove longitudinal tray advancement. The picking device consisted of eight claws that simultaneously gripped eight seedlings. A slotted-track mechanism increased the claw spacing from the picking spacing to the dropping spacing. The extracted seedlings were then dropped into seedling distribution cups arranged in a ring for rotary distribution.

Table 1 compares six representative seedling picking and dropping systems in terms of picking rate per row, success rate, number of picking claws, tray handling method, and distribution method. Unreported values are marked as NR.

Table 1. Comparison of representative seedling picking and dropping systems.

System	Picking Rate (Seedlings·min^{-1}·row^{-1})	Success Rate (%)	Number of Picking Claws	Tray Conveying Method	Distribution Method
Yao et al. [23]	50–60	Average seedling picking success rate: 95	6	Stepwise tray conveying	Fixed distribution tubes
Jin et al. [24]	60/90/120	92.59/87.41/77.78, respectively (picking)	1	Two-axis tray indexing using a lead screw and double-chain conveyor	Direct dropping into planting mechanism
Han et al. [25]	NR (manipulator transplanting rate: 1000–1200 seedlings·h^{-1})	94.22 ± 1.62 (tomato); 95.16 ± 1.39 (pepper); 96.41 ± 1.18 (cabbage), for transplanting	1	Chain-driven tray conveying	Direct transfer to destination pots
Ma et al. [26]	18	98.08	6 or 8	Stepwise tray conveying	Moving distribution cups
Liu et al. [27]	NR	92.4	8	Stepwise tray conveying	Rotary distribution disk
Li et al. [28]	NR(reported bench operating rates: 100/150/200 seedlings·min^{-1})	97.40/98.44/95.03, respectively (bench picking and depositing)	8	Tray indexing using a ratchet-and-chain mechanism	Rotary distribution cups

Although these systems differ in structural configuration, they commonly employ stepwise tray conveying, whole-row or simultaneous multi-seedling picking, and rotary seedling distribution. These operating methods impose stringent requirements on positioning accuracy and manufacturing and assembly precision. They also involve complex timing coordination and motion matching among seedling supply, picking, dropping, and planting.

To address the numerous operational steps and structural complexity of existing two-row automatic transplanters that employ stepwise tray conveying, whole-row seedling picking with multiple claws arranged side by side, and rotary seedling distribution, an alternating seedling picking and dropping system was developed. The system integrates a stationary seedling tray, alternating picking and dropping by left and right picking claw groups, and alternating seedling feeding by a fixed distribution device. The proposed configuration eliminates the need for stepwise tray conveying during picking and for a rotary seedling distribution mechanism. To achieve precise and efficient seedling picking, a picking path was planned based on the tray cell arrangement and optimized using an S-curve acceleration and deceleration strategy to determine the motion timing parameters for different seedling positions. Based on the seedling receiving the window of the

planting mechanism, spatial and temporal matching relationships were established among seedling picking, seedling dropping, and the operation of the planting mechanism. The continuous operation sequence for an entire tray was calculated to determine the parameters and time margins at each picking position. Timing coordination within the seedling picking and dropping system was then analyzed to select operating parameters within the investigated ranges.

2. Materials and Methods

2.1. Structure and Working Principle of the Two-Row Automatic Transplanter

The structure of the two-row automatic transplanter (2ZBA-2C, Zhenjiang, China) is shown in Figure 1. It mainly consists of a rotary tray supply mechanism, an automatic seedling picking and dropping mechanism, seedling distribution tubes, a linkage planting mechanism, and a tracked chassis. These components operate in coordination according to a predefined sequence to achieve continuous tray supply, seedling picking and dropping, seedling distribution, planting, and soil covering.

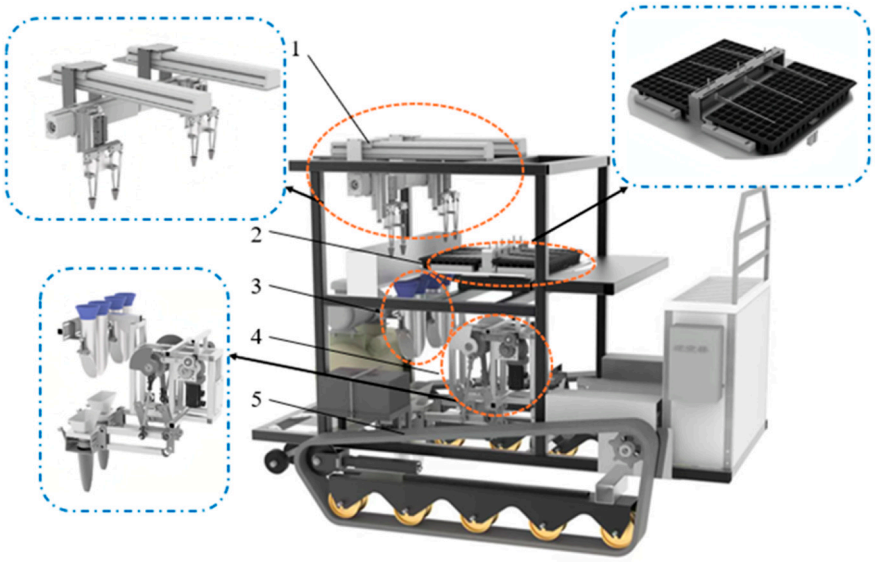

Figure 1. Overall structure of the two-row automatic transplanter. 1. Automatic seedling picking and dropping mechanism; 2. Rotary tray supply mechanism; 3. Seedling distribution tubes; 4. Linkage planting mechanism; 5. Tracked chassis.

The rotary tray supply mechanism uses a servo-driven gear pair that rotates in both directions to alternately switch the trays between the storage area and the picking area. The seedling picking and dropping mechanism precisely picks seedlings in an alternating sequence and drops them into the seedling distribution tubes for temporary buffering. The tubes feed seedlings at coordinated intervals as the planting units reach their seedling receiving positions. The linkage planting mechanism then places the seedlings into the soil, after which the soil-covering mechanism covers the root plugs and compacts the surrounding soil to complete transplanting.

2.2. Structure and Working Principle of the Dual-Module Rapid Alternating Seedling Picking and Dropping System

Common vegetable seedling trays have either 72 cells (6 rows × 12 columns) or 128 cells (8 rows × 16 columns), as shown in Figure 2. Both tray types have overall dimensions of 540 mm × 280 mm, with cell center-to-center spacings of 43 mm and 32.3 mm, respectively.

Three cell spacings in a 72-cell tray are approximately equal to four cell spacings in a 128-cell tray, providing a basis for selecting the spacing between the picking claws.

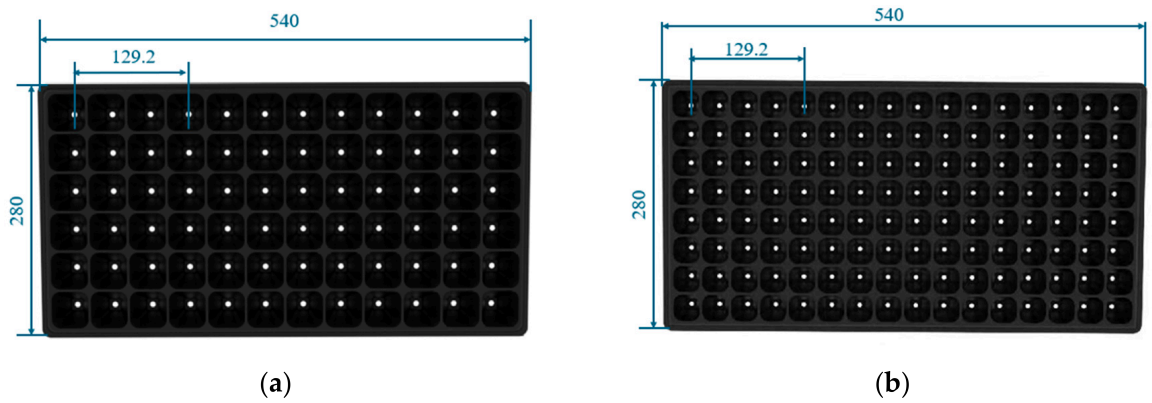

Figure 2. Schematic of plug tray specification (**a**) 72-cell tray. (**b**) 128-cell tray.

The overall structure of the dual-module rapid alternating seedling supply, picking, and dropping system is shown in Figure 3. It mainly consists of a seedling picking and dropping device, a supporting tray supply device, and seedling distribution tubes. The picking and dropping device comprises left and right assemblies, each consisting of transverse and longitudinal linear motion modules, a picking cylinder, a lifting cylinder, and a seedling picking end effector. Each end effector is equipped with two picking claws spaced 129.2 mm apart. The claws adopt an existing two-finger, four-needle design [29]. The linear motion modules drive the end effectors back and forth in the transverse and longitudinal directions within the horizontal plane. The lifting cylinder provides vertical motion, while the picking cylinder actuates claw opening and closing. The supporting rotary tray supply mechanism is located below the picking device and consists of a rotary platform, tray hold-down rods, positioning blocks, and other components. It accommodates both 72-cell and 128-cell trays, supports the seedling trays, and indexes them intermittently to bring the next tray into the picking position. The seedling distribution tubes receive the plug seedlings released by the picking modules and intermittently feed them to the planting mechanism in a predefined sequence.

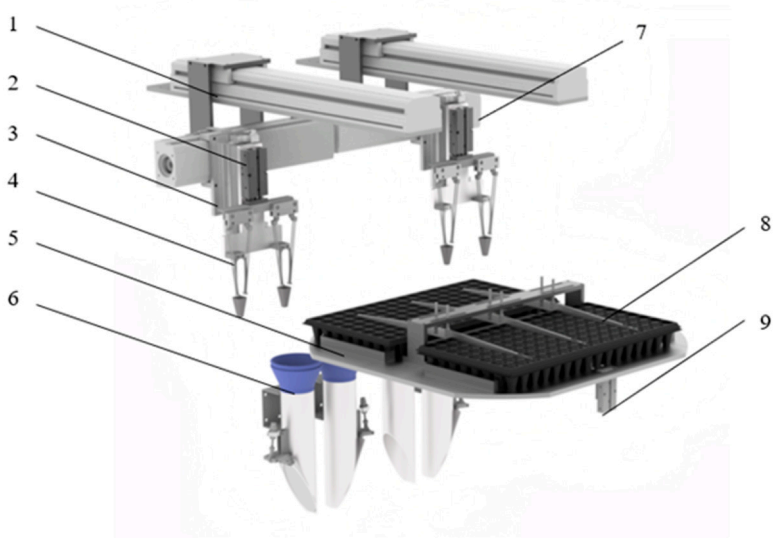

Figure 3. Overall structure of the seedling picking and dropping mechanism. 1. Longitudinal picking module; 2. Picking cylinder; 3. Lifting cylinder; 4. Picking needles; 5. Positioning block; 6. Seedling distribution tube; 7. Transverse picking module; 8. Seedling pressing rod; 9. Positioning cylinder.

During operation, the rapid alternating seedling picking and dropping system of the two-row automatic transplanter keeps the tray stationary and adjusts the positions of the picking claws according to the target cells. Once the tray is in position, the four picking claws in the left and right assemblies move from above the seedling distribution tubes to above the target cells through simultaneous actuation of the transverse and longitudinal linear motion modules. They simultaneously extract four plug seedlings, with the two claws in each assembly spaced three cell pitches apart for 72-cell trays or four cell pitches apart for 128-cell trays, and then return to the distribution tubes to drop the seedlings. The planting mechanism receives one seedling at a time, while the tubes holding the remaining three seedlings open and close sequentially according to the planting frequency.

After each dropping operation, the linear motion modules move the picking claws one cell pitch to the right of the previous picking positions within the same row. When advancing to the next row, the claws return to the first column of their respective picking areas. This sequence is repeated until all seedlings in the tray have been picked. Owing to the operating characteristics of the planting mechanism, the left duckbill planting unit consistently completes planting before the right unit. To improve efficiency, the left and right assemblies begin alternating seedling picking after the second planting operation and continue until the entire tray has been emptied.

2.3. Seedling Picking Motion Planning and Control Strategy Design

2.3.1. Seedling Picking and Dropping Path Planning

To meet the requirements for continuous seedling supply and spatial and temporal coordination during automatic transplanting, a two-station rotary tray-changing mechanism was adopted to supply trays alternately. Using a 128-cell tray as an example, a picking path planning strategy was developed based on spatial partitioning for paired picking claws. Each seedling picking end effector is equipped with two claws maintained at a fixed transverse spacing corresponding to four cell pitches. This spacing enables the claws to pick seedlings from separated cells within the same row. After all seedlings in the current row have been picked, the end effector advances longitudinally to the next row and repeats the picking sequence.

A seedling picking and dropping path was adopted in which each tray is divided into two working zones and seedlings are picked from spaced cells in a left-to-right sequence. To reduce transverse travel and improve picking efficiency, the picking sequence was optimized according to the claw spacing and tray cell arrangement. Figure 4 illustrates the planned picking and dropping path. Based on the spatial coverage of the picking claws, each row is divided into left and right working zones. The left picking claw group handles seedlings in columns 1–8, while the right group handles those in columns 9–16. Each seedling distribution tube feeds seedlings from four columns. During system startup, the two modules simultaneously pick and drop the first batch of four seedlings, initially filling all distribution tubes. The picking modules then immediately return to the tray to pick the next batch. As the first batch is fed sequentially in the order of left tube 1, right tube 1, left tube 2, and right tube 2, both left distribution tubes become empty before both right tubes. The left picking device therefore performs its next picking and dropping operation first, with a phase difference of half a planting cycle relative to the right module. From the third picking cycle onward, a staggered alternating operation pattern gradually develops, as shown in Figure 5, enabling continuous coordination of seedling picking, dropping, feeding, receiving, and planting.

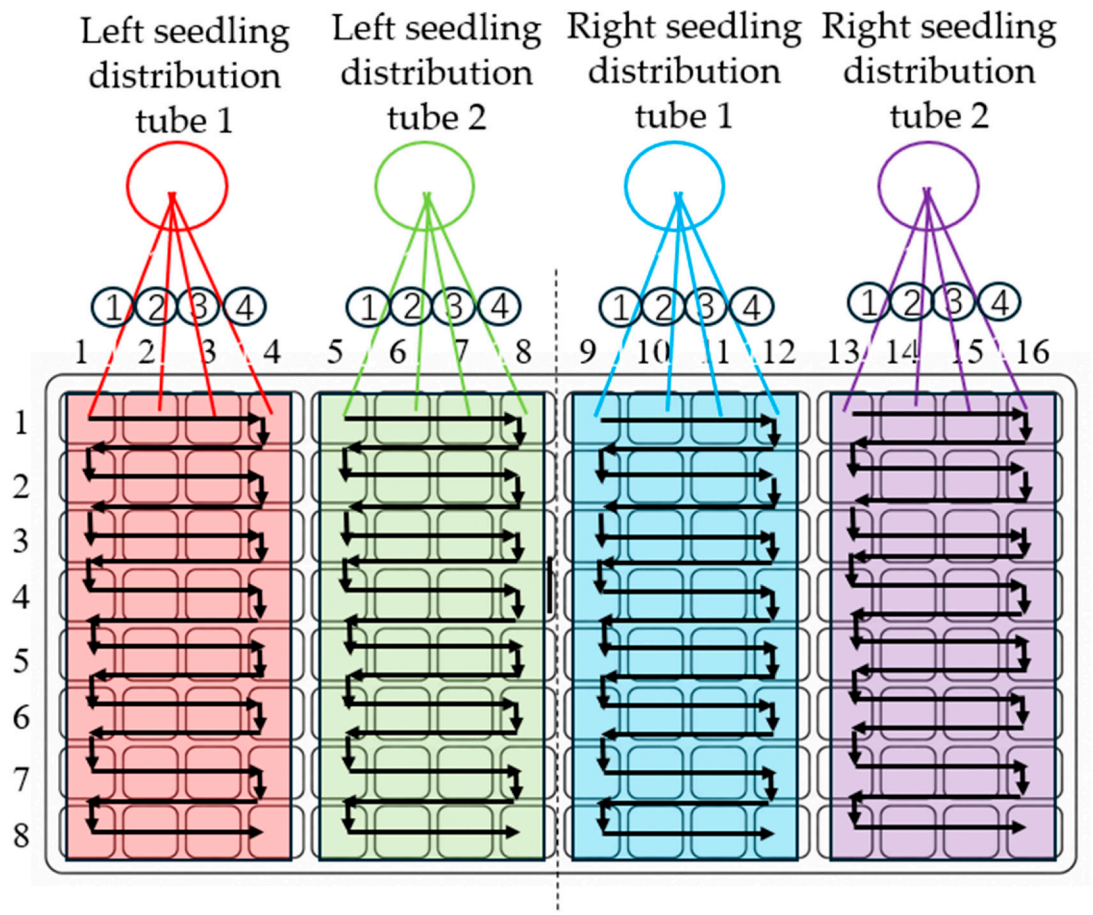

Figure 4. Schematic of path planning for seedling picking and dropping.

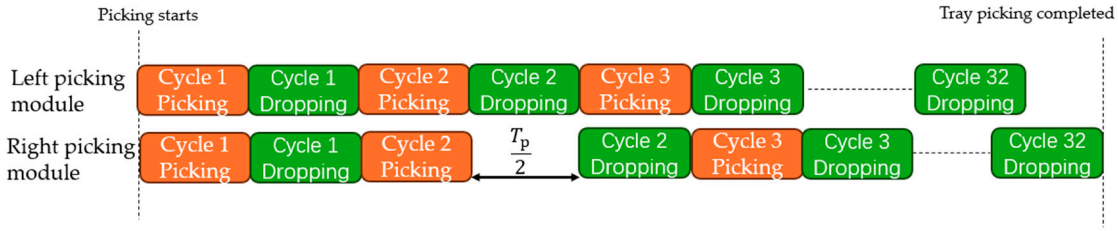

Figure 5. Schematic of alternating seedling picking and dropping.

2.3.2. S-Curve Acceleration and Deceleration Control Strategy for Seedling Transfer

During automatic transplanting, the picking mechanism must complete positioning relative to the tray, seedling picking, and return travel to the dropping position within a limited time. Conventional trapezoidal velocity profiles involve abrupt changes in acceleration during startup and stopping, which can cause substantial mechanical shock and vibration and compromise picking positioning accuracy. In contrast, S-curve acceleration and deceleration profiles maintain continuous velocity and acceleration during servo motor operation, reducing mechanical shock and improving motion smoothness [30]. Therefore, an S-curve acceleration and deceleration control strategy was adopted to plan the motion trajectories of the dual-module picking mechanism, improve motion smoothness, and reduce mechanical shock during continuous reciprocating motion.

Jerk was introduced as a constraint to ensure continuous variation in acceleration. As shown in Figure 6, a complete S-curve velocity profile comprises seven distinct phases, from

increasing acceleration to decreasing deceleration, ensuring smooth motion throughout the cycle.

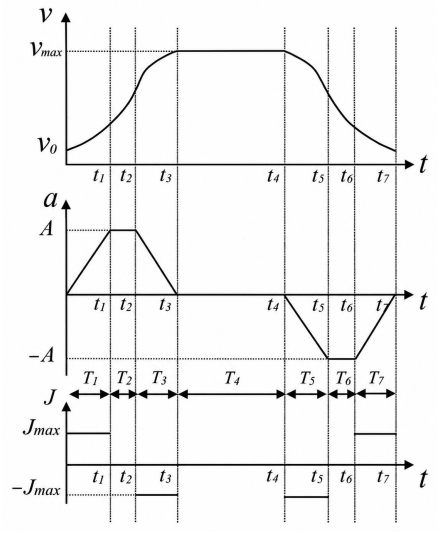

Figure 6. Schematic of the S-curve acceleration and deceleration profile.

During seedling picking, the short travel distance prevents the actuator from reaching the prescribed maximum velocity. Deceleration must therefore begin before this velocity is reached, eliminating the constant-velocity phase and producing a six-phase S-curve profile. The six phases comprise increasing acceleration, constant acceleration, decreasing acceleration, increasing deceleration, constant deceleration, and decreasing deceleration; thus, $T_4 = 0$.

The picking travel distance depends on the row containing the target plug seedling. Considering the maximum motor-driven travel velocity of 1000 mm/s and allowing a velocity margin, the velocity limit was set to 900 mm/s. The maximum acceleration was calculated from the required acceleration time and set to 3000 mm/s^2. The maximum jerk was set to 20,000 mm/s^3 to balance motion responsiveness and smoothness. These parameters serve as constraints for the subsequent S-curve trajectory planning. The motion parameters, determined through theoretical calculations and consideration of agronomic requirements, are listed in Table 2. These values represent motion constraints, whereas the actual peak velocity and acceleration depend on the travel distance. For the investigated distances, the peak velocity remained below $V_{\max}$; therefore, no constant-velocity phase was required.

Table 2. Motion parameters of the picking module.

Parameter	Symbol	Design Value
Maximum picking travel	S	350 mm
Maximum allowable velocity	$V_{\max}$	900 mm/s
Maximum acceleration	$A_{\max}$	3000 mm/s^2
Maximum jerk	$J_{\max}$	20,000 mm/s^3

For a symmetric six-phase S-curve acceleration and deceleration profile, the phase durations are related as follows:

(1) Duration of the increasing-acceleration phase T_1:

$$T_1 = \frac{A_{\max}}{J_{\max}} \quad (1)$$

(2) The displacement S and the duration of the constant-acceleration phase T_2 satisfy the following relationship:

The displacement constraint is obtained by summing the displacements over the three acceleration phases. The displacement during the increasing-acceleration phase is given by:

$$S_1 = \int_0^{T_1} \frac{1}{2} J_{\max} t^2 dt = \frac{1}{6} J_{\max} T_1^3 \tag{2}$$

The displacement during the constant-acceleration phase is given by:

$$S_2 = \int_0^{T_2} (\frac{1}{2} A_{\max} T_1 + A_{\max} \mathrm{t}) dt = \frac{1}{2} A_{\max} T_1 T_2 + \frac{1}{2} A_{\max} T_2^2 \tag{3}$$

(3) The displacement during the decreasing-acceleration phase is given by:

$$S_3 = \int_0^{T_3} (\frac{1}{2} A_{\max} T_1 + A_{\max} \mathrm{T}_2 + A_{\max} \mathrm{t} - \frac{1}{2} \mathrm{J}_{\max} \mathrm{t}^2) dt = \frac{5}{6} A_{\max} T_1^2 + A_{\max} T_1 T_2 \tag{4}$$

Thus, the total displacement during the acceleration stage is given by:

$$S_{\mathrm{acc}} = A_{\max} T_1^2 + \frac{3}{2} A_{\max} T_1 T_2 + \frac{1}{2} A_{\max} T_2^2 \tag{5}$$

Because the motion profile is symmetric, the total displacement is $S = 2S_{\mathrm{acc}}$. Substituting $T_1 = A_{\max}/J_{\max}$ yields the following relationship:

$$S = \frac{2{A_{\max}}^3}{{J_{\max}}^2} + \frac{3{A_{\max}}^2}{J_{\max}} T_2 + A_{\max} T_2^2 \tag{6}$$

Thus, the duration of the constant-acceleration phase, T_2 is obtained as:

$$T_2 = \frac{\sqrt{\frac{{A_{\max}}^2}{{J_{\max}}^2} + \frac{4S}{A_{\max}}} - \frac{3A_{\max}}{J_{\max}}}{2} \tag{7}$$

(4) The total motion duration T is given by:

$$T = 2(2T_1 + T_2) \tag{8}$$

(5) Peak velocity V_{p}:

$$V_P = \frac{1}{2} A_{\max} T_1 + A_{\max} T_2 + \frac{1}{2} A_{\max} T_3 = A_{\max}(T_1 + T_2) \tag{9}$$

The calculated values were $T_1 = 0.15$ s, $T_2 = 0.125$ s, $T = 0.849$ s, and $V_{\mathrm{p}} = 824$ mm/s. For the maximum picking travel distance of 350 mm, the planned peak velocity was approximately 824 mm/s, below the prescribed velocity limit of 900 mm/s. Thus, $V_{\mathrm{p}} < V_{\max}$, indicating that no constant-velocity phase was required under this operating condition. The velocity constraint was therefore satisfied, confirming the suitability of the six-phase S-curve profile.

The steady-state cycle duration comprises travel from the distribution tubes to the target tray cells, return travel, and two pneumatic stages. The X- and Y-axis motions are performed simultaneously. The maximum Y-axis travel distance is 64.6 mm, corresponding to two tray cell pitches. Under the specified Y-axis motion profile, the calculated maximum travel time is approximately 0.333 s, shorter than the minimum X-axis travel time of 0.583 s. Therefore, transverse motion does not add a separate time component.

The pneumatic actions comprise two sequential stages, with the lifting and picking cylinders actuated simultaneously during seedling release. The allocated duration of 0.200 s per pneumatic stage includes the time required to complete the corresponding gripping or releasing action. Compared with the nominal cylinder action time of approximately 0.150 s,

this allocation provides a timing allowance of 0.050 s per stage for pneumatic response and operating variability. This allowance is included in the cycle calculation rather than added separately. The steady-state cycle time is therefore calculated as:

$$T_{cycle} = 2T + 2t_p \tag{10}$$

In the formula, T—One-way X-axis travel time, s; t_p—Design time allocated to each pneumatic stage, taken as 0.200 s.

No additional programmed dwell is included in this calculation. Waiting for the distribution tubes to become available is treated separately in the timing coordination analysis.

The longitudinal picking travel distance varies among tray rows because each row is located at a different distance from the picking reference position. The spacing between adjacent rows is 32.3 mm, and the longitudinal travel distances for rows 1–7 are 123.9 mm, 156.2 mm, 188.5 mm, 220.8 mm, 253.1 mm, 285.4 mm, and 317.7 mm, respectively. S-curve trajectory parameters were determined for each travel distance to ensure that the velocity, acceleration, and jerk constraints were satisfied at all picking positions.

The minimum travel distance required for a six-phase S-curve profile is given by:

$$S_c = 2\frac{A_{max}^3}{J_{max}^2} \tag{11}$$

For $(S < S_c)$, the motion parameters are calculated as follows:

$$\begin{gathered} T_1 = \left(\frac{S}{2J_{max}}\right)^{1/3} \\ A_p = J_{max}T_1 \\ V_p = J_{max}T_1^2 \\ T = 4T_1 \end{gathered} \tag{12}$$

Substituting the parameter values yields $S_c = 135$ mm. Since the travel distance for the first row is 123.9 mm, which is less than S_c, a short-distance S-curve profile without constant-acceleration or constant-deceleration phases is used $(T_2 = 0\ \text{s})$. In this case, T_1 is reduced to 0.146 s, $A_p = 2915.4\ \text{mm/s}^2$, $V_p = 425.0$ mm/s, $T = 0.583$ s and the peak acceleration remains below the prescribed limit A_{max}. For rows 2–8, the maximum acceleration is reached, and six-phase S-curve acceleration and deceleration profiles with constant-acceleration and constant-deceleration phases are adopted.

2.4. Timing Coordination Analysis of the Seedling Picking and Dropping System

During the initial stage, the left and right modules pick seedlings simultaneously and drop four plug seedlings into the seedling distribution tubes. However, the left and right planting mechanisms complete planting at different times. Subsequent picking operations are therefore controlled according to the planting completion status rather than a fixed actuation sequence. After releasing a pair of seedlings, each picking module immediately returns to the tray to pick the next pair. Upon arrival at the dropping position, the module waits, if necessary, until both corresponding distribution tubes have emptied and returned to their closed positions before releasing the two seedlings simultaneously. This enables dynamic coordination between the picking and dropping process and the planting completion status. Each module returns to the tray immediately after releasing its seedlings. Subsequent seedling release is permitted only after both corresponding distribution tubes have emptied and returned to their closed positions.

The end effector of the linkage planting mechanism follows an approximately horizontal trajectory near its uppermost position, providing a stable region for receiving plug seedlings. The time interval during which the end effector traverses this trajectory segment

is defined as the seedling receiving window, as shown in Figure 7. Within this window, seedlings can be received stably with minimal disturbance.

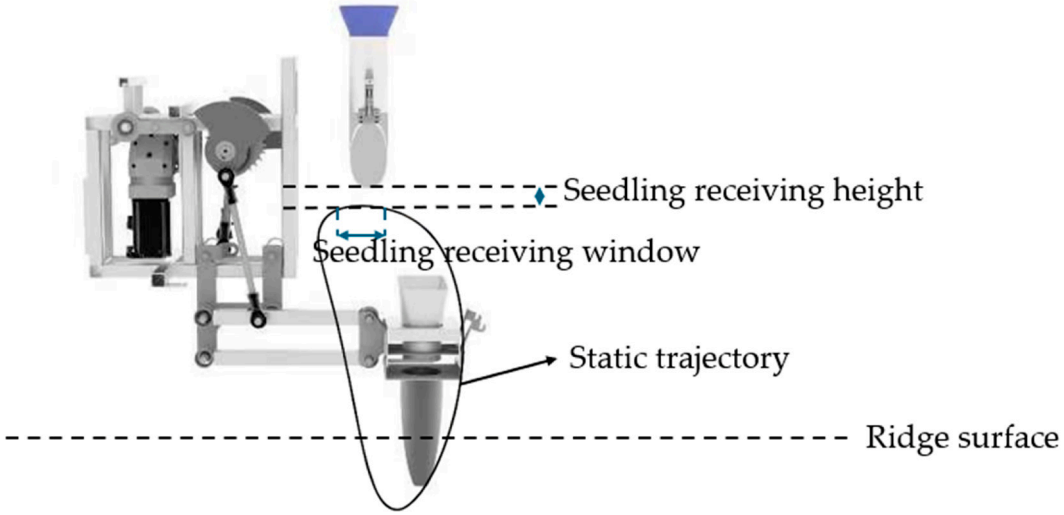

Figure 7. Schematic of spatiotemporal matching between the seedling distribution tube and the planting mechanism.

Timing coordination in the seedling picking and dropping system centers on spatial and temporal matching between seedling feeding and receiving. This requires synchronizing the distribution tube opening instant with the seedling receiving window of the planting end effector and matching the seedling release height with the receiving height. These relationships ensure that seedlings accurately enter the receiving region of the planting mechanism within the appropriate time interval and height range.

The system therefore employs a dynamic timing coordination mechanism for dual-module seedling picking and dropping, driven by planting completion. The module corresponding to the side that completes planting first is triggered first, allowing picking and dropping operations to adapt to the planting completion status. This reduces waiting time associated with a fixed operating schedule and improves operational continuity and time utilization.

To verify timing coordination during continuous operation over an entire tray, the complete picking, dropping, and receiving sequence was calculated individually for all 128 seedlings. The instant when the picking claws reached the dropping position during the second picking cycle was defined as the time reference ($t = 0$). The distribution tube opening instant was defined as the elapsed time from this reference instant until the tube reached its fully open position. The pneumatic actuator of the distribution tube was controlled by a Xinje XD5 PLC (Wuxi Xinje Electric Co., Ltd., Wuxi, China), using its built-in 1 ms timer to provide a timing setting resolution of 1 ms. Under stable air supply pressure, the timing repeatability of the fully open instant was within ±5 ms.

Based on the motion sequences of the dual-module picking and dropping mechanism and the planting mechanism, the picking, dropping, and receiving times were calculated for each seedling.

To evaluate timing coordination between the dual-module picking and dropping system and the planting mechanism at different picking positions, the picking and dropping time margin was defined as the difference between the interval available for successive picking and dropping cycles on the same side and the actual time required to complete a picking and dropping cycle.

The time margins were calculated for each row of the tray to assess the system's ability to maintain coordinated continuous operation at different picking positions.

After release from the seedling distribution tube, the seedling was assumed to undergo free fall from rest under gravity. Friction between the seedling and the tube wall and aerodynamic drag on the seedling, including its leaves, were neglected in this analytical model. The theoretical seedling receiving time was therefore calculated as the sum of the distribution tube opening instant and the free-fall time. A mathematical model describing the relationship among the distribution tube, the plug seedling, and the duckbill planting unit was established as follows:

$$\begin{gathered} T_w = \frac{n_2 - n_1}{360^\circ} T_p \\ H = \frac{1}{2} g t_f^2 \\ T_r = t_0 + t_f \end{gathered} \tag{13}$$

In the formula, T_w—Seedling receiving time window, s; T_p—Planting period, s; n_1, n_2—Planting shaft angles corresponding to the two boundaries of the receiving window near the top dead center, °; H—Seedling receiving height, mm; g—Gravitational acceleration, 9810 mm·s^{-2}; t_f—Free-fall time, s; t_0—Opening instant of the seedling distribution tube, s; T_r—Theoretical seedling receiving time, s.

In theory, accurate seedling receiving requires the predicted receiving time to fall within the seedling receiving window. The coordination accuracy of the entire system is primarily governed by the distribution tube opening instant, planting frequency, and seedling receiving height.

2.5. Motion Simulation and Parameter Optimization of Seedling Feeding and Receiving

2.5.1. Development of the Motion Simulation Model

A three-dimensional parametric simulation model of the seedling feeding and receiving system was developed to visually assess the feasibility of the mechanism design and investigate the spatial and temporal coupling between seedling release and the receiving motion of the duckbill planting unit, thereby avoiding interference or missed seedling receiving. To simulate the relative spatial positions of the plug seedling and the duckbill planting unit after release from the distribution tube during transplanting, a mechanical simulation model was constructed in RecurDyn 2024 (FunctionBay, Inc., Seongnam, Republic of Korea) , as shown in Figure 8. The motion paths of the plug seedling and the duckbill planting unit were analyzed to identify where their trajectories intersected and thereby determine the optimal seedling release position parameters.

At the beginning of each simulation, the plug seedling was positioned vertically above the seedling distribution tube with zero initial velocity. The planting mechanism was initialized at a phase at which the left and right duckbill planting units were at the same vertical height. The distribution tube opening instant followed the time reference defined in Section 2.4. The simulation duration was set to 2 s, with the number of simulation steps set to 300. The maximum and initial integration time steps were 1×10^{-3} s and 1×10^{-6} s, respectively. The error tolerance was set to 5×10^{-3}, and the numerical damping parameter was set to 1.

During the simulation, the seedling was modeled as a rigid body, with its mass and inertia properties specified as shown in Figure 9a. "Solid Contact" properties were specified to model collisions between the plug seedling and the seedling distribution tube. The contact parameters were specified based on the measurements reported in [31], and the corresponding settings are shown in Figure 9b. The "Show Trace" function was used to track the seedling's center of mass and record its coordinates under different operating conditions. This trajectory visualization enabled analysis of the kinematic characteristics of the falling seedling and assessment of the coordination accuracy between the mechanisms.

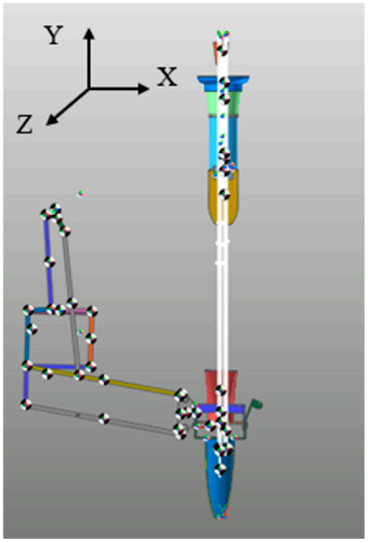

Figure 8. Motion model.

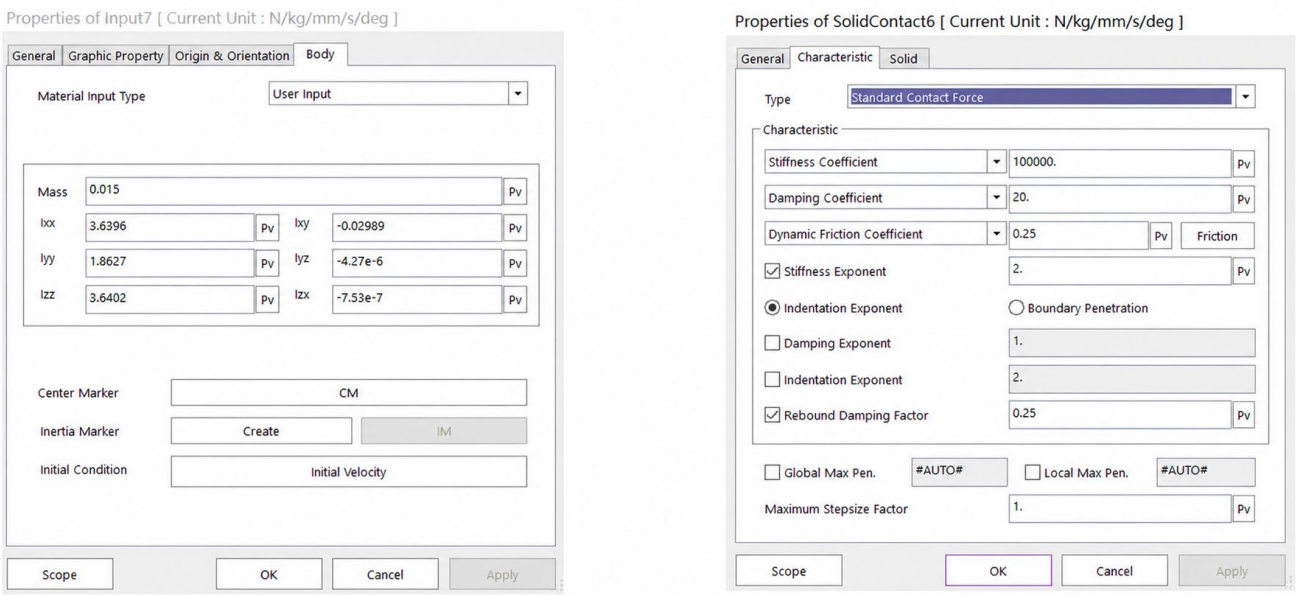

Figure 9. Simulation model parameters (**a**) Mass and inertia properties of the plug seedling. (**b**) Solid contact parameters between the plug seedling and the seedling distribution tube.

2.5.2. Single-Factor Experiments

In the RecurDyn simulation coordinate system, the *X*-axis represents the horizontal direction in the plane of the planting mechanism motion, whereas the *Z*-axis is perpendicular to this plane. Alignment in the Z-direction is primarily determined by installation and assembly and was not varied in the present parameter optimization. Horizontal landing deviation along the *X*-axis was selected as the response variable because the falling seedling must enter the finite receiving opening of the moving duckbill planting unit. Near its uppermost position, the duckbill follows an approximately horizontal trajectory within the receiving window. The horizontal offset between the seedling center and the duckbill center therefore quantifies their alignment during reception.

Vertical motion also affects successful reception by influencing the timing and position at which the falling seedling encounters the moving duckbill. In this study, vertical motion was included through the simulated seedling falling trajectory and the prescribed motion of

the planting mechanism, with seedling receiving height included as an optimization factor. Changes in receiving height alter the seedling fall time and consequently the horizontal position of the duckbill at seedling arrival, as discussed in Section 3.3.1. Thus, horizontal landing deviation was used to quantify receiving alignment under the modeled conditions, rather than as a complete criterion for successful reception. Actual receiving performance was evaluated separately using the seedling receiving success rate in the machine tests.

To assess seedling feeding and receiving performance, the "Distance" function in the "Result" module of RecurDyn was used to measure the displacement deviation between the center of the plug seedling and the center of the duckbill planting unit along the horizontal axis, defined as the X-axis in the simulation coordinate system. This deviation provides a quantitative indication of their alignment during seedling receiving and was calculated as follows:

$$D_x = \left| X_p - X_q \right| \tag{14}$$

In the formula, X_p—Horizontal coordinate (X-axis) of the root plug center, mm; X_q—Horizontal coordinate (X-axis) of the duckbill center, mm.

To investigate the effect of the distribution tube opening instant on seedling receiving accuracy, single-factor timing simulations were conducted at a planting frequency of 50 seedlings per row per minute and a seedling receiving height of 50 mm. The distribution tube opening instant was varied to obtain the seedling landing positions under different timing conditions. Performance was evaluated based on whether the landing point fell within the effective receiving area of the duckbill planting unit and its positional deviation from the duckbill center.

To investigate the effect of planting frequency on seedling receiving performance, single-factor timing simulations were conducted at a seedling receiving height of 50 mm and a distribution tube opening instant of 0.57 s. Seven planting frequency levels ranging from 44 to 56 seedlings per row per minute were tested. The seedling landing position was obtained at each frequency, and its positional deviation from the geometric center of the duckbill planting unit was used to quantify receiving alignment.

To investigate the effect of seedling receiving height, single-factor timing simulations were conducted at a planting frequency of 50 seedlings per row per minute and a distribution tube opening instant of 0.57 s. The receiving height was varied incrementally from 0 to 200 mm. The seedling falling trajectory and landing position on the duckbill receiving plane were obtained at each height. Receiving alignment was evaluated using the positional deviation between the seedling landing point and the geometric center of the duckbill planting unit.

The simulations focused on spatial and temporal matching between seedling feeding from the distribution tubes and seedling receiving by the duckbill planting units. The seedling picking and dropping process was not included. Therefore, the planting frequencies considered in these simulations were used to investigate seedling feeding and receiving performance and did not establish the continuous operating capability of the complete machine.

2.5.3. Multifactor Experiments

To optimize spatial and temporal coordination during seedling feeding and receiving, a three-factor, three-level Box–Behnken design was adopted. Distribution tube opening instant, planting frequency, and seedling receiving height were selected as the factors, and seedling landing point deviation was used as the response variable to quantify seedling receiving accuracy. The factor ranges were determined from the single-factor simulations, and the coded levels are listed in Table 3. The design comprised 17 simulation runs, including

five center-point runs, and was used to evaluate the linear, quadratic, and interaction effects of the factors on seedling receiving performance.

Table 3. Factor levels and coding.

Coded Level	A: Opening Instant of the Seedling Distribution Tube (s)	B: Planting Frequency (Seedlings·row^{-1}·min^{-1})	C: Seedling Receiving Height (mm)
−1	0.56	48	25
0	0.57	50	50
1	0.58	52	75

The relationships between the coded factors and their physical values were defined as follows:

$$\begin{aligned} A &= \frac{t_0 - 0.57}{0.01} \\ B &= \frac{f - 50}{2} \\ C &= \frac{H - 50}{25} \end{aligned} \quad (15)$$

In the formula, A—Dimensionless coded factor for distribution tube opening instant; B—Dimensionless coded factor for planting frequency; C—Dimensionless coded factor for seedling receiving height; t_0—Distribution tube opening instant, s; f—Planting frequency, seedlings·row^{-1}·min^{-1}; H—Seedling receiving height, mm.

2.6. Performance Tests of the Seedling Picking and Dropping System

2.6.1. Experimental Equipment and Materials

The 2ZBA-2C fully automatic vegetable transplanter is shown in Figure 10a. Standard 128-cell rigid plastic seedling trays measuring 280 × 540 × 43 mm were used. The cabbage seedlings were grown for 35 days and ranged from 110 to 130 mm in height, as shown in Figure 10b. The growing substrate consisted of peat, vermiculite, and perlite mixed at a volumetric ratio of 3:1:1, with a moisture content of approximately 60%. The tests were conducted in Suzhou and Yangzhou, Jiangsu Province, China.

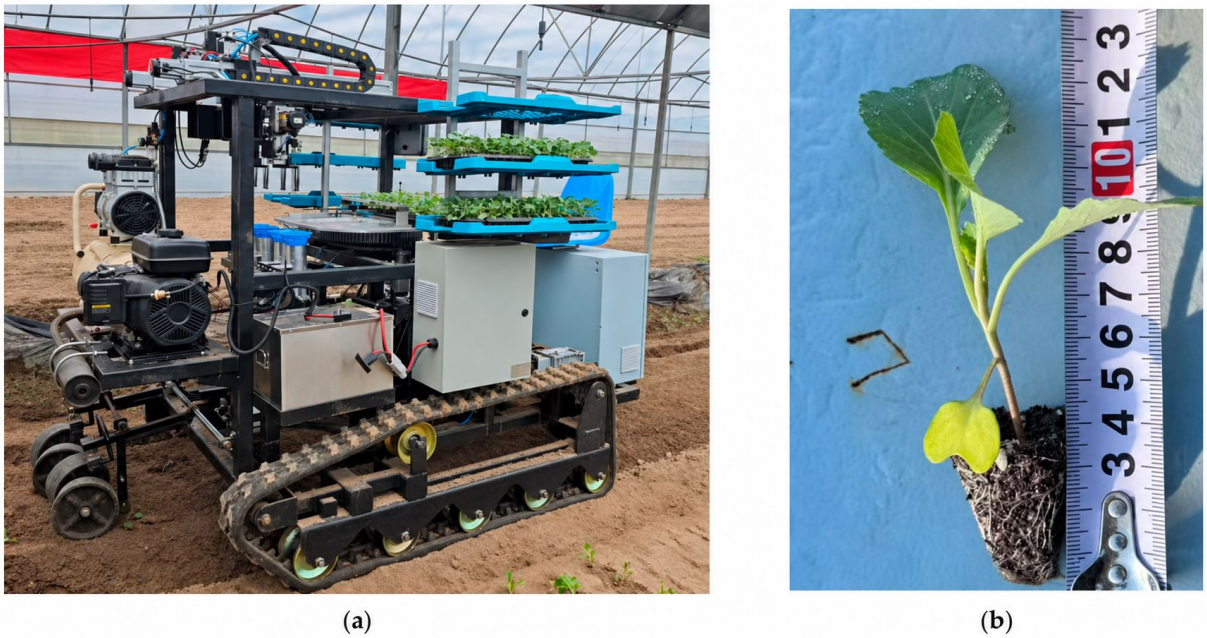

Figure 10. Experimental equipment and materials (**a**) 2ZBA-2C fully automatic vegetable transplanter. (**b**) Seedlings used in the experiments.

The rotary tray supply mechanism was designed to accommodate both 72-cell and 128-cell trays. In this study, only 128-cell trays were used for performance testing because their smaller cell dimensions impose more demanding requirements on picking positioning accuracy. Therefore, the reported picking and dropping success rate applies to 128-cell trays; picking and dropping performance with 72-cell trays was not experimentally evaluated.

2.6.2. Experimental Procedure and Evaluation Metrics

Performance tests of seedling picking, dropping, and receiving were conducted to evaluate the rotary tray supply mechanism and verify the effectiveness of the optimized parameters. During the picking and dropping tests, the travel drive connection was disconnected, and the machine was operated at a stationary position. Rotary tray supply, seedling picking, and seedling dropping were performed sequentially, and the tests were repeated. Successful seedling picking and dropping was defined as the intact extraction of a plug seedling and its successful placement into the seedling distribution tube. The seedling picking and dropping success rate was calculated to evaluate the operational performance of the mechanism.

Full-machine dynamic tests of seedling picking, dropping, and receiving were then conducted (Figure 11). The plant spacing was set to 300 mm, and the machine forward speed was automatically coordinated with the planting frequency to maintain this spacing. Cabbage seedlings were dropped into the distribution tubes in the prescribed order and subsequently received by the planting units in sequence. The mechanism and operating parameters were determined based on the preceding theoretical analysis. A control treatment was also included, with the distribution tube opening instant, planting frequency, and seedling receiving height set to 0.56 s, 54 seedlings per row per min, and 100 mm, respectively, to provide a comparison with the selected parameter combination. The corresponding forward speed settings were 0.255 m/s for the optimized treatment and 0.270 m/s for the control treatment. The complete machine operating sequence was executed to assess the timing coordination of the seedling picking and dropping system during dynamic operation. Because the instantaneous seedling landing position could not be measured precisely during machine operation, the seedling receiving success rate was used as an evaluation metric. Receiving was considered successful when the duckbill planting unit caught the seedling released from the distribution tube; otherwise, it was considered a failure. The receiving success rate was calculated as the number of seedlings successfully received divided by the number actually released from the distribution tubes, expressed as a percentage. Upstream picking and dropping failures that prevented seedlings from reaching the distribution tubes were excluded from this metric and evaluated separately using the picking and dropping success rate.

The seedling picking and dropping success rate and the seedling receiving success rate were used as evaluation metrics. Their respective calculation formulas are given by:

$$\begin{aligned} Q_1 &= \frac{N_1 - a}{N_1} \times 100\% \\ Q_2 &= \frac{N_2 - b}{N_2} \times 100\% \end{aligned} \tag{16}$$

In the formula, N_1—Number of seedlings tested for picking and dropping; a—Number of seedlings that failed to be picked and dropped; N_2—Number of seedlings tested for receiving; b—Number of seedlings that failed to be received.



(**a**) (**b**)

Figure 11. Schematic of the experimental setup (**a**) Seedling picking and dropping test. (**b**) Seedling receiving test.

3. Results and Discussion

3.1. Results of Seedling Picking Motion Planning and Control Strategy Design

The motion parameters were calculated separately for the two travel-distance regimes. For the first tray row ($S < S_c$), the short-distance relationships in Section 2.3.2 were used to calculate the jerk-ramp duration, peak acceleration, peak velocity, and one-way travel time. For rows 2—8 ($S > S_c$), the six-phase relationships were used to determine the constant-acceleration duration and the corresponding peak velocity and travel time. The calculated parameters and achieved motion peaks are summarized in Table 4.

Table 4. Motion parameters for different plug tray rows.

Row Number	Picking Distance (mm)	T_1/s	T_2/s	V_p(mm/s)	A_p(mm/s^2)	J_p(mm/s^3)	T/s	Profile Type
1	123.9	0.146	0	425.0	2915.4	20,000	0.583	Short-distance S-curve
2	156.2	0.150	0.015	495.6	3000	20,000	0.630	Six-phase S-curve
3	188.5	0.150	0.037	559.9	3000	20,000	0.673	Six-phase S-curve
4	220.8	0.150	0.056	619.4	3000	20,000	0.713	Six-phase S-curve
5	253.1	0.150	0.075	675.0	3000	20,000	0.750	Six-phase S-curve
6	285.4	0.150	0.092	727.3	3000	20,000	0.785	Six-phase S-curve
7	317.7	0.150	0.109	776.9	3000	20,000	0.818	Six-phase S-curve
8	350.0	0.150	0.125	824.1	3000	20,000	0.849	Six-phase S-curve

As shown in Table 4, as the seedling picking travel distance increased from 123.9 to 350.0 mm, the duration of the constant-acceleration phase gradually increased from 0 to 0.125 s, the peak velocity increased from 425.0 to 824.1 mm/s, and the total motion duration increased from 0.583 to 0.849 s. For the first row, the short travel distance did not allow

a constant-acceleration phase to develop under the specified maximum acceleration and jerk constraints; therefore, a short-distance S-curve profile was used. For rows 2–8, the longer travel distances allowed a complete six-phase S-curve acceleration and deceleration profile. These results indicate that motion parameters must be adapted to different seedling picking positions by adjusting the duration of the constant-acceleration phase, while velocity, acceleration, and jerk remain within the specified limits.

To further analyze the motion characteristics of the seedling picking module under long-travel conditions, the maximum seedling picking travel distance was simulated in MATLAB R2021a(The MathWorks, Inc., MA, USA). The resulting displacement, velocity, and acceleration curves under the six-phase S-curve acceleration and deceleration control strategy are shown in Figure 12.

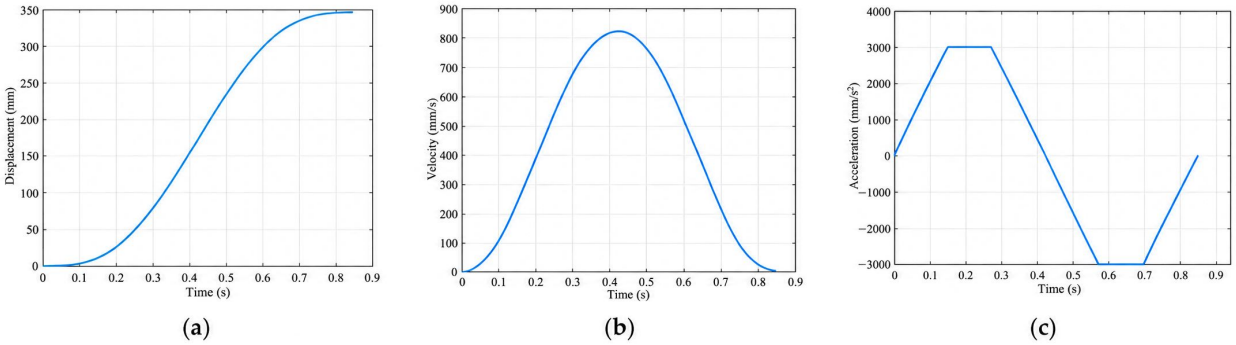

Figure 12. Six- phase S-curve acceleration and deceleration profiles of the picking module (**a**) Displacement profile. (**b**) Velocity profile. (**c**) Acceleration profile.

As shown in Figure 12, the module displacement increases continuously with time, the velocity varies continuously during acceleration and deceleration, and the acceleration transitions continuously between adjacent phases. By imposing piecewise constraints on jerk, the S-curve profile avoids the instantaneous changes in acceleration associated with conventional trapezoidal velocity planning.

Together, Table 4 and Figure 12 indicate that the proposed motion planning method can accommodate different target cells in the seedling tray. The motion duration determined for each cell position provides the basis for designing the timing of dual-module seedling picking and dropping. As the target picking position moves farther from the dropping position, the motion duration increases, directly affecting the time margin available for alternating operation of the two modules. Thus, the motion durations obtained for different tray rows not only support the feasibility of the S-curve motion planning method but also provide the basis for subsequent timing coordination among dual-module seedling picking, seedling dropping, and planting operations. Previous research has shown that appropriate trajectory planning helps improve motion smoothness and reduce mechanical shocks during high-speed operation [32], which is consistent with the results of this study.

3.2. Results of Timing Coordination Analysis for the Seedling Picking and Dropping System

The same seedling picking sequence was used for each tray row: cells 1, 5, 9, and 13 were picked first, followed by cells 2, 6, 10, and 14; cells 3, 7, 11, and 15; and cells 4, 8, 12, and 16. Taking the first row as an example, the timing of seedling picking and dropping by the left and right modules and seedling receiving by the duckbill planting units was analyzed. The complete operating sequence for the 16 seedlings in the first row is presented in Table 5. The per-seedling timing calculations for all 128 tray cells are provided in the Supplementary Materials.

Table 5. Timing parameters of the seedling picking and dropping system for the first tray row.

Picking Cycle	Picking Module	Seedling No.	Arrival Time at the Dropping Position (s)	Entry Time into the Seedling Distribution Tube (s)	Distribution Tube Opening Instant (s)	Remarks
1	Left	1,5	Initially in position	Initially deposited	0.560,1.736	Synchronous picking
1	Right	9,13	Initially in position	Initially deposited	1.148,2.325	Synchronous picking
2	Left	2,6	0	2.136	2.913,4.089	Synchronous picking
2	Right	10,14	0	2.725	3.501,4.678	Synchronous picking
3	Left	3,7	3.502	4.489	5.266,6.442	Staggered left–right operation
3	Right	11,15	4.091	5.078	5.854,7.031	Staggered left–right operation
4	Left	4,8	5.855	6.842	7.619,8.795	Staggered left–right operation
4	Right	12,16	6.444	7.431	8.207,9.384	Staggered left–right operation

As shown in Table 5, the left and right picking modules perform seedling picking and dropping alternately. Each module picks two seedlings simultaneously and drops them into the corresponding seedling distribution tubes. The two modules operate with a time offset, allowing the corresponding channel on one side to continue seedling dropping and receiving while the module on the other side performs picking and return movements. This arrangement allows some operations to overlap in time. As the picking position changes, the times at which the seedlings reach the dropping position and enter the distribution tubes vary accordingly. Nevertheless, during the continuous handling of all 16 seedlings in the first row, seedling feeding is completed within the receiving window of each corresponding duckbill planting unit. These results indicate that the proposed alternating operating mode enables timing coordination during continuous operation within a single tray row.

After releasing a pair of seedlings, each module immediately returns to pick the next pair. If it reaches the dropping position before both corresponding distribution tubes have emptied and recovered, it waits before releasing the two seedlings simultaneously. Thus, the required picking and dropping time excludes waiting, whereas the interval between successive arrivals on the same side includes waiting.

The picking and dropping time margins for all eight tray rows were further analyzed, and the results are presented in Table 6. As the picking travel distance increased from 123.9 to 350.0 mm, the steady-state cycle duration increased from 1.566 to 2.098 s. Based on the longest calculated cycle time of 2.098 s, the theoretical frequency ceiling is approximately 57.2 seedlings per row per minute. With an allowable cycle duration of 2.353 s at the baseline planting frequency of 51 seedlings per row per minute, the time margin gradually decreased from 0.787 to 0.255 s. This increase was primarily attributable to the longer longitudinal round-trip travel distances required for more distant cells. Although higher peak velocities could be reached as the picking travel distance increased, the motion duration still increased with travel distance under the maximum velocity, acceleration, and jerk constraints, resulting in a gradual increase in the picking and dropping cycle duration. The time margin remained positive for every row, indicating that, under the baseline operating conditions, the picking and dropping mechanism could complete each cycle before the next operation on the same side began, thereby meeting the requirements for continuous operation across the entire tray.

Table 6. Time margins for different plug tray rows.

Row Number	Picking Distance (mm)	Steady-State Cycle Time (s)	Allowable Cycle Time (s)	Time Margin (s)
1	123.9	1.566	2.353	0.787
2	156.2	1.660	2.353	0.693
3	188.5	1.746	2.353	0.607
4	220.8	1.826	2.353	0.527
5	253.1	1.900	2.353	0.453
6	285.4	1.970	2.353	0.383
7	317.7	2.036	2.353	0.317
8	350.0	2.098	2.353	0.255

Previous studies on automatic transplanting have shown that coordination among operations such as seedling picking, conveying, and dropping [33,34] is essential for continuous transplanting. The above timing analysis indicates that the dual-module alternating seedling picking and dropping system can maintain timing coordination among picking, dropping, and planting operations during continuous handling of both the 16 seedlings in a single tray row and all eight rows of the tray. It also indicates that the motion durations obtained for different cell positions in Section 3.1 can be effectively used for subsequent timing coordination of seedling picking and dropping. Compared with a single picking module that sequentially performs picking, dropping, and return movements, the proposed system alternates picking and dropping between the left and right modules, allowing some mechanism movements to be staggered in time and thereby providing the necessary time margin for continuous seedling feeding.

3.3. Results of Seedling Feeding and Receiving Motion Simulation and Parameter Optimization

3.3.1. Results of Single-Factor Experiments

Because of the limited seedling receiving window, deviations in the distribution tube opening instant, planting frequency, or seedling receiving height from their appropriate ranges can cause plug seedlings to land outside the effective receiving area of the duckbill planting unit, resulting in receiving failures. Typical receiving failures are shown in Figure 13.

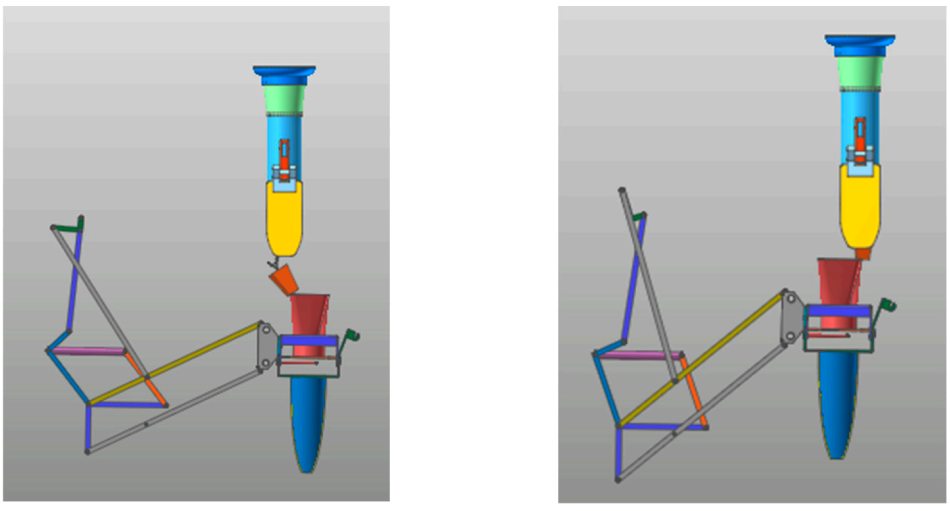

(**a**) (**b**)

Figure 13. Schematic of typical seedling receiving failures (**a**) leftward landing deviation. (**b**) rightward landing deviation.

The distribution tube opening instant has a marked influence on the seedling landing position. As shown in Figure 14, when the distribution tube opens before 0.53 s or after 0.61 s, the plug seedling lands outside the effective receiving area of the duckbill planting unit, preventing successful seedling receiving. The opening instant determines when the plug seedling begins to fall freely and therefore alters the phase relationship between its arrival at the receiving plane and the position of the moving duckbill planting unit. If the tube opens too early, the seedling reaches the receiving area before the duckbill planting unit reaches a suitable position. If it opens too late, the duckbill planting unit may have already passed the optimal receiving region. Both conditions result in a failure of timing coordination.

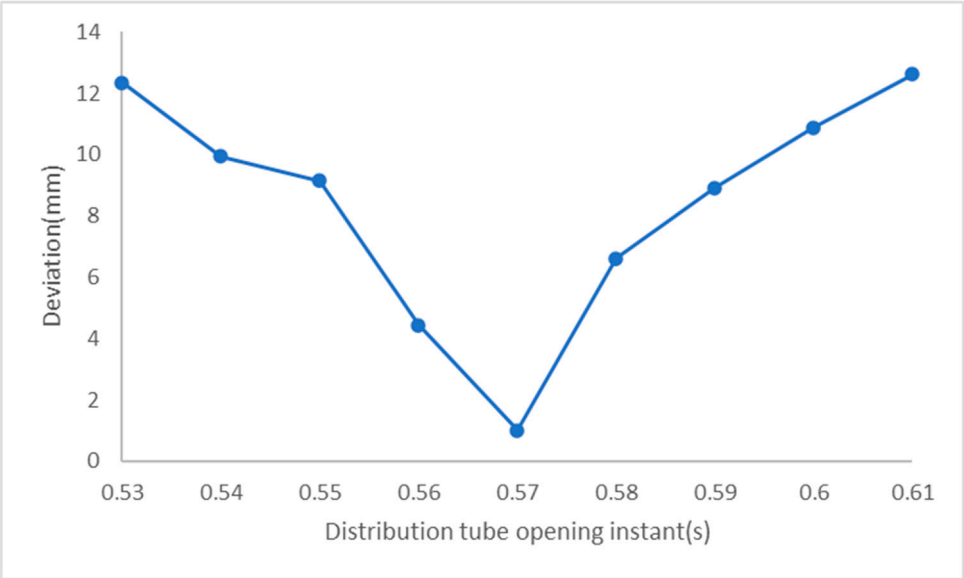

Figure 14. Effect of the opening instant of the seedling distribution tube on landing deviation.

Further analysis of the simulation results showed that the spatial deviation between the seedling landing point and the center of the duckbill planting unit was small when the distribution tube opening instant was within 0.56–0.58 s. This result indicates that stable seedling receiving depends not only on whether the plug seedling enters the duckbill opening but also on phase matching between the seedling's fall and the periodic motion of the duckbill planting unit. Therefore, the distribution tube opening instant should be set in coordination with the motion cycle of the planting mechanism.

As shown in Figure 15, at a seedling receiving height of 50 mm and a distribution tube opening instant of 0.57 s, the seedling landing point deviation first decreased and then increased with increasing planting frequency. The positional deviation between the seedling landing point and the geometric center of the duckbill planting unit was small at planting frequencies of 48–52 seedlings per row per minute and gradually increased as the frequency moved outside this range. This occurred because planting frequency altered both the motion velocity of the duckbill planting unit and the time at which it reached the receiving position. With the distribution tube opening instant held constant, changes in planting frequency altered the relative phase between the seedling's fall and the motion of the duckbill planting unit, resulting in a suitable frequency range for seedling receiving.

With the initial seedling dropping conditions held constant, increasing the seedling receiving height increased the free-fall distance of the plug seedling and consequently prolonged its fall time. During this period, the duckbill planting unit continued to move along its prescribed trajectory. Its horizontal position therefore changed when the seedling reached the receiving plane, causing the seedling landing position relative to the duckbill

center to shift from left to right as the receiving height increased. This result indicates that seedling receiving height primarily affects spatial matching by altering the free-fall time of the plug seedling.



Figure 15. Effect of planting frequency on landing deviation.

As shown in Figure 16, when the seedling receiving height was within 25–75 mm, the positional deviation between the seedling landing point and the duckbill center was relatively small. Taken together, the three single-factor experiments indicate that the distribution tube opening instant and planting frequency primarily alter the relative timing of seedling release and receiving, whereas the receiving height changes the free-fall time and thereby affects the relative spatial position at the receiving plane. Thus, seedling feeding and receiving performance is jointly constrained by temporal and spatial matching. The three parameters should therefore be determined together, providing a basis for the subsequent multifactor response surface analysis.

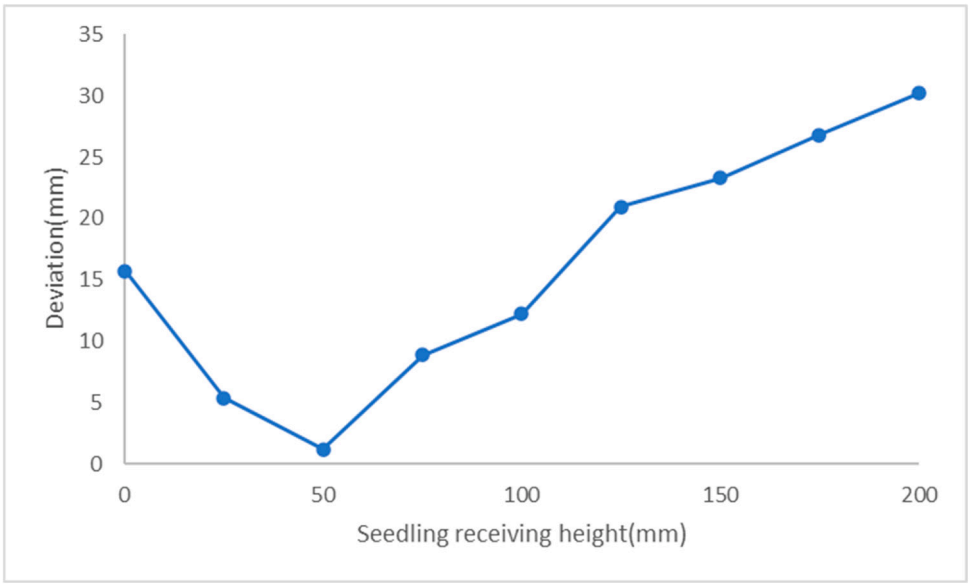

Figure 16. Effect of seedling receiving height on landing deviation.

3.3.2. Results of Multifactor Experiments and Analysis of Variance

The single-factor simulation results indicated that relatively suitable parameter ranges existed for the distribution tube opening instant, planting frequency, and seedling receiving height. Accordingly, reasonable ranges and center levels were selected for each factor, considering both computational efficiency and the trends observed in the single-factor simulations. Seventeen experimental conditions were established. The parameter settings and the simulated seedling landing point deviations from the geometric center of the duckbill planting unit are presented in Table 7.

Table 7. Box–Behnken experimental design and results.

Run No.	A (Coded)	B (Coded)	C (Coded)	Landing Deviation (mm)
1	1	0	1	13.74
2	0	0	0	0.5
3	−1	1	0	2.06
4	0	−1	−1	6.72
5	0	0	0	0.9
6	−1	−1	0	8.64
7	0	0	0	1.8
8	1	−1	0	2.7
9	0	0	0	1.2
10	−1	0	−1	5.61
11	0	0	0	1.5
12	0	1	−1	4.53
13	0	−1	1	11.95
14	1	1	0	10.5
15	1	0	−1	2.95
16	0	1	1	12.12
17	−1	0	1	5.11

A Box–Behnken design comprising 17 simulation runs, including five nominal center-point runs, was generated using Design-Expert 13 (Stat-Ease, Inc., Minneapolis, MA, USA). For each run, the specified factor settings were applied in RecurDyn, and the seedling landing point deviation was recorded.

Multiple regression analysis and analysis of variance were performed on the experimental data using Design-Expert. With seedling landing point deviation as the response and distribution tube opening instant (A), planting frequency (B), and seedling receiving height (C) as the factors, the fitted quadratic polynomial regression model is given by:

$$Y = 1.18 + 1.06A - 0.1B + 2.89C + 3.6AB + 2.82AC + 0.59BC + 1.41A^2 + 3.39B^2 + 4.26C^2 \quad (17)$$

The significance of the regression model and its coefficients was evaluated, and the results are presented in Table 8.

As shown in Table 8, the overall regression model was highly significant ($p < 0.0001$), indicating a significant statistical association between the deviation and the three factors within the experimental range. Among the linear terms, distribution tube opening instant (A; $p = 0.0079$) and seedling receiving height (C; $p < 0.0001$) were significant and highly significant, respectively, whereas planting frequency (B; $p = 0.7386$) was not significant. However, B^2 was highly significant, indicating that the effect of planting frequency on the deviation was not simply linear but exhibited pronounced curvature. This finding is consistent with the initial decrease and subsequent increase in deviation observed in the single-factor experiment as planting frequency increased. As shown in Figure 17, The interaction terms AB and AC were highly significant, indicating marked coupling between

distribution tube opening instant and both planting frequency and seedling receiving height. The former reflects the need to coordinate the opening instant with the motion cycle of the duckbill planting unit, whereas the latter reflects the need to adjust the opening instant to compensate for changes in free-fall time caused by variations in receiving height.

Table 8. Significance tests and analysis of variance (ANOVA) for the landing deviation model.

Source	Sum of Squares	df	Mean Square	F-Value	*p*-Value
Model	306.59	9	34.07	51.33	<0.0001
A—Opening instant of the seedling distribution tube	8.97	1	8.97	13.51	0.0079
B—Planting frequency	0.08	1	0.08	0.1205	0.7386
C—Seedling receiving height	66.76	1	66.76	100.6	<0.0001
AB	51.70	1	51.7	77.9	<0.0001
AC	31.87	1	31.87	48.02	0.0002
BC	1.39	1	1.39	2.10	0.1907
A^2	8.36	1	8.36	12.59	0.0094
B^2	48.28	1	48.28	72.75	<0.0001
C^2	76.55	1	76.55	115.34	<0.0001
Residual	4.65	7	0.6636		
Corrected total	311.24	16			

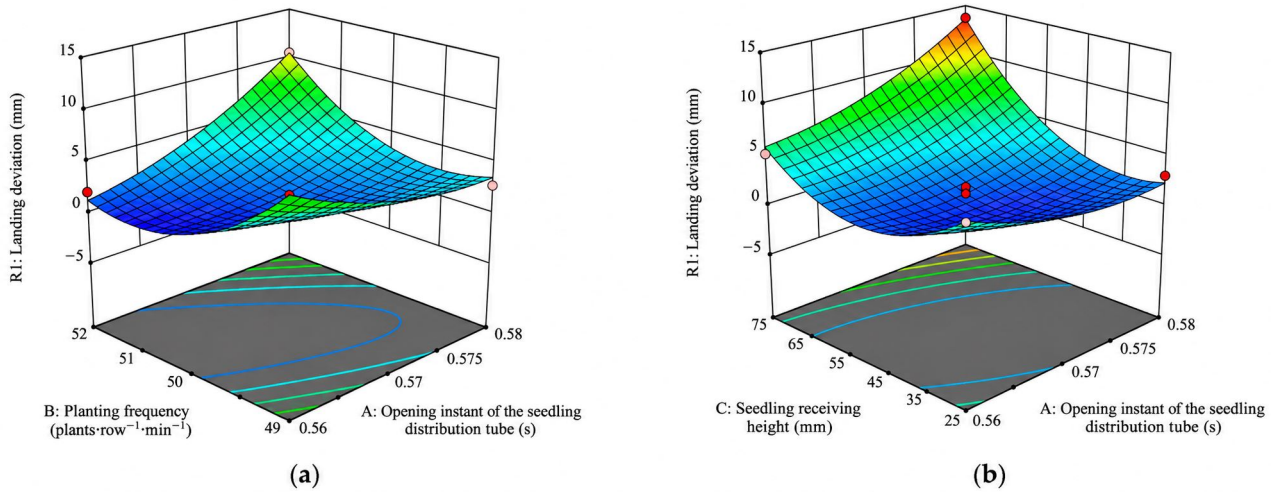

Figure 17. Response surfaces of seedling landing point deviation. (**a**) Interaction between distribution tube opening instant and planting frequency. (**b**) Interaction between distribution tube opening instant and seedling receiving height.

These statistical results should be interpreted with caution because the variation among the nominal center-point runs was not independently characterized. The reported significance levels are conditional on the assumptions of the regression analysis and do not independently establish model adequacy or the robustness of the predicted optimum. The fitted model was therefore used as an approximate description of the simulated responses within the investigated parameter range.

The fit statistics for the quadratic regression model are summarized in Table 9. The R^2, adjusted R^2, and predicted R^2 values were 0.9851, 0.9659, and 0.8089, respectively. The CV was 14.97%, and the adequate precision was 19.9145. Residual diagnostic plots are presented in Figure 18. The square markers represent individual simulation runs and are colored according to the landing point deviation, ranging from blue (low values) to red (high values). The red diagonal line in (a) is the normal reference line. The red horizontal

lines in (b) indicate the diagnostic limits displayed by the software (±4.81963), and the black horizontal line indicates zero residual. The externally studentized residuals approximately followed the reference line in the normal probability plot, although some deviations were observed. The residuals-versus-predicted plot showed no clear funnel-shaped pattern, but negative residuals were clustered at intermediate predicted values, suggesting possible local model discrepancies. These statistics and diagnostic plots describe the fit and predictive performance estimated from the simulation dataset and should be interpreted subject to the limitations associated with the unexplained center-point variation.

Table 9. Fit statistics for the quadratic regression model of seedling landing point deviation.

Statistic	Value
R2	0.9851
Adjusted R^2	0.9659
Predicted R^2	0.8089
CV (%)	14.97
Adequate precision	19.9145

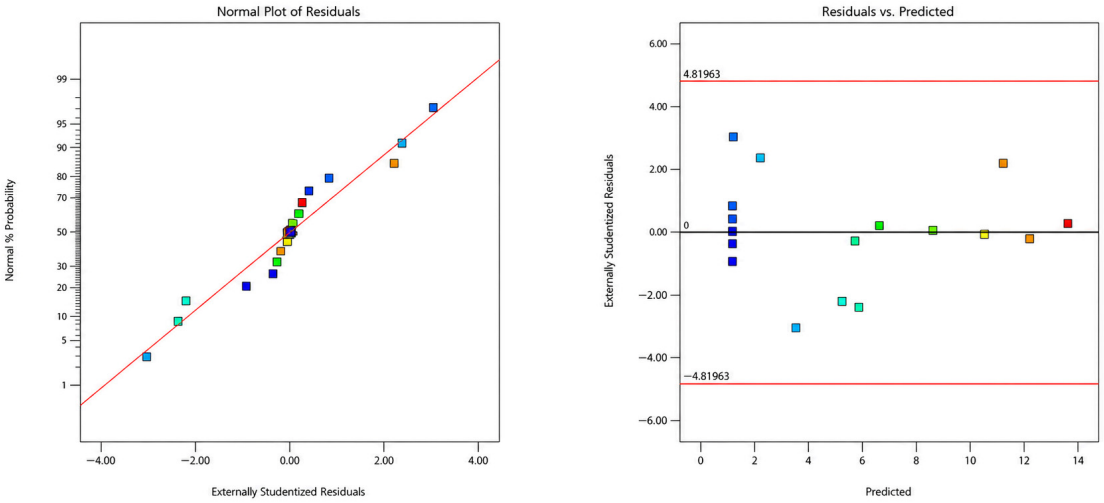

Figure 18. Residual diagnostics for the quadratic regression model. (**a**) Normal probability plot of externally studentized residuals. (**b**) Externally studentized residuals versus predicted values.

3.3.3. Selection of Operating Parameters

Numerical optimization was performed using the fitted quadratic regression model to identify operating parameter combinations associated with small seedling landing point deviations within the investigated ranges. A distribution tube opening instant of 0.56 s, a planting frequency of 51 seedlings per row per minute, and a nominal seedling receiving height of approximately 49 mm (rounded from the model output of 48.86 mm) were selected for subsequent machine tests. This combination represents a model-based selection within the investigated ranges, rather than a confirmed global optimum. Because the reported opening instant was at the lower design boundary, improved parameter combinations outside the investigated ranges cannot be excluded.

In practical operation, planting frequency is prescribed according to agronomic requirements and the target work rate. Its inclusion in the present analysis was intended to investigate its interaction with distribution tube opening instant and seedling receiving height. The selected combination therefore applies to the investigated operating condition and should not be interpreted as a universal recommendation for other planting frequencies.

No additional simulation was conducted to independently confirm the predicted minimum deviation. The machine tests evaluated seedling receiving success and supported the operational feasibility of the selected combination, but did not validate the predicted minimum deviation. In addition, an allowable tolerance for seedling receiving height was not established in this study.

The single-factor and multifactor analyses indicate that distribution tube opening instant, planting frequency, and seedling receiving height do not affect seedling feeding and receiving performance independently. Rather, they jointly determine the matching between the seedling's arrival at the receiving area and the motion state of the planting mechanism. The single-factor experiments identified appropriate ranges for the parameters, while the multifactor analysis further revealed their interactions and provided the basis for determining the selected parameter combination. This finding is consistent with previous research showing that coordinating seedling feeding parameters with the motion state of the planting mechanism improves seedling receiving performance during transplanting [35]. In this study, distribution tube opening instant, planting frequency, and seedling receiving height were incorporated into a unified optimization framework. Using seedling receiving deviation as the evaluation metric, the system parameters were jointly optimized in terms of timing coordination and spatial conditions for seedling receiving.

3.4. Results of Performance Tests for the Seedling Picking and Dropping System

3.4.1. Results and Analysis of Seedling Picking and Dropping Tests

Seedling picking and dropping tests were conducted consecutively on six trays, each containing 128 seedlings. The results are presented in Table 10. Across the six trials, 741 of the 768 seedlings were successfully picked and dropped, yielding an overall seedling picking and dropping success rate of 96.48%. The success rates across the six trials ranged from 95.31% to 97.66%. The third trial had the lowest success rate, at 95.31%. During the tests, some seedlings were observed to have bent stems that overlapped with neighboring seedlings, causing adjacent seedlings to be pulled along during picking. This may have interfered with the normal extraction and dropping of plug seedlings. These observations suggest that seedling morphology and growth conditions within the tray may be among the factors affecting the overall seedling picking and dropping success rate.

Table 10. Seedling picking and dropping test data.

Test No.	Total Number of Seedlings per Tray	Number of Seedlings Successfully Picked and Dropped	Picking and Dropping Success Rate (%)
1	128	123	96.09
2	128	123	96.09
3	128	122	95.31
4	128	124	96.88
5	128	124	96.88
6	128	125	97.66

The absence of quantitative root plug strength measurements and failure counts by category limits the identification of the relative contributions of seedling properties and mechanism operation to unsuccessful attempts.

Comparison with the performance results reported in References [23–28] suggests that the proposed system achieves a favorable balance between operating throughput and seedling picking and dropping success. At a controller-set planting frequency of 51 seedlings

per row per minute, the two-row system achieved an overall picking and dropping success rate of 96.48%.

3.4.2. Results and Analysis of Seedling Receiving Success Rate Tests

Field planting tests were conducted using the complete machine with the selected parameter combination determined in Section 3.3. The numbers of seedlings released from the seedling distribution tubes and successfully received by the duckbill planting units were recorded. The results are presented in Tables 11 and 12. The seedling receiving success rate was 100% in all trials under the selected parameter combination, with all 300 seedlings successfully received. In the control treatment, 293 of 300 seedlings were successfully received, yielding an overall receiving success rate of 97.67%. The optimized treatment therefore achieved a receiving success rate 2.33 percentage points higher than that of the control treatment. These results support the feasibility of the selected parameter combination for coordinating seedling feed and reception under the tested conditions. However, the observed receiving success rate of 100% represents zero receiving failures among the 300 seedlings tested and does not establish failure-free performance across other operating conditions or during prolonged operation. Further tests with larger samples and a broader range of operating conditions are needed to assess receiving reliability.

Table 11. Seedling receiving success rate test data for the control treatment.

Test No.	Number of Seedlings Tested for Receiving	Number of Seedlings Successfully Received	Seedling Success Receiving Rate (%)
1	40	40	100
2	40	39	97.5
3	50	49	98
4	50	48	96
5	60	58	96.67
6	60	59	98.33

Table 12. Seedling receiving success rate test data for the selected parameter combination.

Test No.	Number of Seedlings Tested for Receiving	Number of Seedlings Successfully Received	Seedling Success Receiving Rate (%)
1	40	40	100
2	40	40	100
3	50	50	100
4	50	50	100
5	60	60	100
6	60	60	100

4. Conclusions

(1) An alternating seedling picking and dropping system was developed for a two-row automatic transplanter. The system combines stationary trays during picking, two picking modules with two claws each, and fixed seedling distribution tubes. This configuration avoids stepwise tray conveying during picking and rotary seedling distribution. To enable precise and efficient seedling picking, a kinematic model of the picking mechanism was established, the picking path was planned, and an S-curve acceleration and deceleration control strategy was applied to optimize the entire motion process.

(2) A picking path was planned according to the tray cell arrangement, and S-curve motion profiles were determined for different picking distances. The calculated one-way

motion time increased from 0.583 to 0.849 s as the picking distance increased from 123.9 to 350 mm, while satisfying the prescribed velocity, acceleration, and jerk constraints.

(3) Timing calculations were performed for all 128 tray cells. At a planting frequency setting of 51 seedlings per row per minute, the calculated steady-state picking and dropping cycle times ranged from 1.566 to 2.098 s, with corresponding time margins of approximately 0.787 to 0.255 s. These results indicate timing feasibility under the assumed motion sequence and allocated pneumatic action times.

(4) The effects of distribution tube opening instant, planting frequency, and seedling receiving height on seedling landing point deviation were investigated through RecurDyn simulations. Single-factor experiments and multifactor simulation experiments based on a Box–Behnken design identified a selected parameter combination: a distribution tube opening instant of 0.56 s, a planting frequency of 51 seedlings per row per minute, and a seedling receiving height of approximately 49 mm. Separate machine tests yielded a picking and dropping success rate of 96.48% and a receiving success rate of 100% among the 300 seedlings tested under the selected receiving conditions. These findings provide a theoretical basis for the design and parameter optimization of two-row automatic transplanters.

Supplementary Materials: The following supporting information can be downloaded at: https://www.mdpi.com/article/10.3390/agronomy16212202/s1, Table S1: Per-seedling timing calculations for all 128 cells of the plug tray.

Author Contributions: Conceptualization, J.S. and J.H.; methodology, J.S., J.H. and X.C.; software, J.S., W.L. and Q.Y.; validation, J.S., X.C. and H.W.; formal analysis, J.S. and Z.Z.; investigation, J.S. and J.H.; resources, J.H. and X.C.; data curation, J.S. and W.L.; writing—original draft preparation, J.S.; writing—review and editing, J.H., X.C., W.L. and Q.Y. All authors have read and agreed to the published version of the manuscript.

Funding: This research was funded by the Ministry of Agriculture and Rural Affairs of the People's Republic of China through National Key Science and Technology Project for Agriculture (NK202216030303) and the Department of Agriculture and Rural Affairs of Jiangsu Province through the project Development of Key Technologies and Equipment for Efficient Automatic Transplanting of Open-Field Cabbage (NJ2024-04).

Data Availability Statement: The original contributions presented in this study are included in the article/supplementary material. Further inquiries can be directed to the corresponding author.

Conflicts of Interest: The authors declare no conflicts of interest.

References

1. Lin, Z.; Li, X.; Sun, H.; Zhou, M.; Yin, J.; He, J.; Yin, D. Design and Experimental Validation of Stem-Clamping-and-Pull-out-Type Pepper Plug Seedling-Picking Mechanism. *Agriculture* **2025**, *15*, 1563. [CrossRef]
2. Cheng, B.; Wu, H.; Zhu, H.; Liang, J.; Miao, Y.; Cui, Y.; Song, W. Current Status and Analysis of Key Technologies in Automatic Transplanters for Vegetables in China. *Agriculture* **2024**, *14*, 2168. [CrossRef]
3. Khadatkar, A.; Sawant, C.P.; Magar, A.P.; Kumar, V. Agricultural Robots and Automated Machinery for Handling of Nursery Seedlings with Special Reference to the Transplanting Devices. *Discov. Appl. Sci.* **2025**, *7*, 916. [CrossRef]
4. Jin, Y.; Liu, J.; Xu, Z.; Yuan, S.; Li, P.; Wang, J. Development Status and Trend of Agricultural Robot Technology. *Int. J. Agric. Biol. Eng.* **2021**, *14*, 1–19. [CrossRef]
5. Chen, M.; Xu, Y.; Han, C.; Yuan, P.; Shi, Z.; You, J.; Li, D.; Ma, X.; Mao, H. A Machine-Vision Based Seedling Replenishing System for Pepper Plug Seedling Transplanter. *Comput. Electron. Agric.* **2026**, *252*, 112080. [CrossRef]
6. Iqbal, M.Z.; Islam, M.N.; Park, T.; Kim, Y.-J.; Chung, S.-O. Working Speed Analysis of the Gear-Driven Dibbling Mechanism of a 2.6 kW Walking-Type Automatic Pepper Transplanter. *Machines* **2021**, *9*, 6. [CrossRef]
7. Chen, M.; Xu, Y.; Han, C.; Li, D.; Yang, B.; Qiu, S.; Luo, Y.; Mao, H.; Ma, X. Design and Testing of Miniaturized Electrically Driven Plug Seedling Transplanter. *Agriculture* **2025**, *15*, 1589. [CrossRef]

8. Han, C.; Hu, X.; Zhang, J.; You, J.; Li, H. Design and Testing of the Mechanical Picking Function of a High-Speed Seedling Auto-Transplanter. *Artif. Intell. Agric.* **2021**, *5*, 64–71. [CrossRef]
9. Cui, Z.; Fu, J.; Li, J.; Ji, H.; Wu, C.; Zheng, S.; Xiao, T.; Chen, Y.; Zhang, C.; Yang, Y.; et al. Design and Test of the Progressive Push-out Automatic Seedling-Taking Device for Vegetable Substrate Block Seedlings. *Int. J. Agric. Biol. Eng.* **2025**, *18*, 89–100. [CrossRef]
10. Sharma, A.; Narang, M.K.; Chaudhary, D. Attribute-Based Coding of Vegetable Seedling Transplanting Machine. *J. Agr. Eng.-India* **2023**, *60*, 329–339. [CrossRef]
11. Ye, B.; Zeng, G.; Deng, B.; Yang, C.; Liu, J.; Yu, G. Design and Tests of a Rotary Plug Seedling Pick-up Mechanism for Vegetable Automatic Transplanter. *Int. J. Agric. Biol. Eng.* **2020**, *13*, 70–78. [CrossRef]
12. Khadatkar, A.; Pandirwar, A.P.; Paradkar, V. Design, Development and Application of a Compact Robotic Transplanter with Automatic Seedling Picking Mechanism for Plug-Type Seedlings. *Sci. Rep.* **2023**, *13*, 1883. [CrossRef] [PubMed]
13. Magar, A.P.; Nalawade, S.M.; Walunj, A.A.; Khadatkar, A.; Bhangare, S.C.; Bhalekar, M.N.; Nimbalkar, C.A.; Gaikwad, B.B. Engineering Properties of Some Plug-Type Vegetable Seedlings for Development of Automatic Vegetable Transplanter. *J. Agr. Eng.-India* **2023**, *60*, 1–13. [CrossRef]
14. Han, L.; Mo, M.; Gao, Y.; Ma, H.; Xiang, D.; Ma, G.; Mao, H. Effects of New Compounds into Substrates on Seedling Qualities for Efficient Transplanting. *Agronomy* **2022**, *12*, 983. [CrossRef]
15. Sharma, A.; Khar, S. Current Developments in Vegetable Transplanters in Developing Countries: A Comprehensive Review. *Int. J. Veg. Sci.* **2022**, *28*, 417–440. [CrossRef]
16. Zhou, B.; Miao, H.; Guan, C.; Ji, X.; Wang, X. Design and Test of Seedling-Picking Mechanism of Fully Automatic Transplanting Machine. *Appl. Sci.* **2024**, *14*, 9235. [CrossRef]
17. Khadatkar, A.; Mathur, S.M.; Gaikwad, B.B. Automation in Transplanting: A Smart Way of Vegetable Cultivation. *Curr. Sci.* **2018**, *115*, 1884–1892. [CrossRef]
18. Wang, L.; Lin, Z.; Zhou, Z.; Yu, G.; Yang, Z.; Yu, X.; Ye, B. Design and Experiment of a Vegetable Plug Seedling Planting Mechanism Combining Non-Circular Gear System and Multi-Link. *Int. J. Agric. Biol. Eng.* **2025**, *18*, 124–134. [CrossRef]
19. Zhou, M.; Shan, Y.; Xue, X.; Yin, D. Theoretical Analysis and Development of a Mechanism with Punching Device for Transplanting Potted Vegetable Seedlings. *Int. J. Agric. Biol. Eng.* **2020**, *13*, 85–92. [CrossRef]
20. Liu, J.Z.; Zhao, S.Y.; Li, N.; Faheem, M.; Zhou, T.; Cai, W.J.; Zhao, M.Z.; Zhu, X.Y.; Li, P.P. Development and Field Test of an Autonomous Strawberry Plug Seeding Transplanter for Use in Elevated Cultivation. *Appl. Eng. Agric.* **2019**, *35*, 1067–1078. [CrossRef]
21. Zhou, M.; Sun, H.; Xu, X.; Yang, J.; Wang, G.; Wei, Z.; Xu, T.; Yin, J. Study on the Method and Mechanism of Seedling Picking for Pepper (*Capsicum annuum* L.) Plug Seedlings. *Agriculture* **2024**, *14*, 11. [CrossRef]
22. Wen, Y.; Zhang, J.; Tian, J.; Duan, D.; Zhang, Y.; Tan, Y.; Yuan, T.; Li, X. Design of a Traction Double-Row Fully Automatic Transplanter for Vegetable Plug Seedlings. *Comput. Electron. Agric.* **2021**, *182*, 106017. [CrossRef]
23. Yao, M.; Lv, J.; Wang, L.; Yue, R.; Hu, J. Cooperative Operation Method of Seedling Conveying and Picking by Full-Automatic Transplanter Based on Multi-Sensor Combination. *Comput. Electron. Agric.* **2024**, *225*, 109311. [CrossRef]
24. Jin, X.; Li, D.; Ma, H.; Ji, J.; Zhao, K.; Pang, J. Development of Single Row Automatic Transplanting Device for Potted Vegetable Seedlings. *Int. J. Agric. Biol. Eng.* **2018**, *11*, 67–75. [CrossRef]
25. Han, L.; Zhang, M.; Wang, Y.; Ma, G.; Yang, Q.; Liu, Y. Design and Tests of a Large-Opening Flexible Seedling Pick-up Gripper with Multiple Grasping Pins. *Agronomy* **2025**, *15*, 1634. [CrossRef]
26. Ma, G.; Mao, H.; Han, L.; Liu, Y.; Gao, F. Reciprocating Mechanism for Whole Row Automatic Seedling Picking and Dropping on a Transplanter. *Appl. Eng. Agric.* **2020**, *36*, 751–766. [CrossRef]
27. Liu, F.; Ji, D.; Meng, Q.; Luo, H.; Li, J.; Guo, M.; Tian, S. Design of an Automatic Seedling Feeding Device for a Single-Disc Vegetable Transplanter. *INMATEH-Agric. Eng.* **2025**, *77*, 987–997. [CrossRef]
28. Li, G.; Xu, Y.; Han, C.; Liang, J.; Luo, Y.; Mao, H.; Cao, G. Design and Experiment of the Follow-up Seedling Picking and Depositing Mechanism for the Pepper Plug Seedling Transplanter. *Agriculture* **2025**, *15*, 2026. [CrossRef]
29. Pan, J.; Chen, F.; Yue, R.; Yao, M.; Li, J. Simulation Optimization and Experiment of Finger-clamping Seedling Picking Claw Based on EDEM-Recurdyn. *Trans. Chin. Soc. Agric.* **2022**, *53*, 75–85. [CrossRef]
30. Wu, H.-M.; Chen, C.-W.; Nian, C.-Y. Experimental Validation of Positioning Control for an X-Y Table Using S-Curve Velocity Trajectory. *Machines* **2025**, *13*, 363. [CrossRef]
31. Shi, J.; Hu, J.; Liu, W.; Yao, M.; Zhou, J.; Zhang, P. Simulation and Parameter Optimization of Inserting-Extracting-Transporting Process of a Seedling Picking End Effector Using Two Fingers and Four Needles Based on EDEM-MFBD. *Plants* **2026**, *15*, 291. [CrossRef] [PubMed]
32. Guo, T.; Li, J.; Zhang, Y.; Cai, L.; Li, Q. Study on Trajectory Optimization for a Flexible Parallel Robot in Tomato Packaging. *Agriculture* **2024**, *14*, 2274. [CrossRef]

33. Khadatkar, A.; Mathur, S.M. Design and Development of an Automatic Vegetable Transplanter Using a Novel Rotating Finger Device with Push-Type Mechanism for Plug Seedlings. *Int. J. Veg. Sci.* **2022**, *28*, 121–131. [CrossRef]
34. Yang, Q.; Huang, G.; Shi, X.; He, M.; Ahmad, I.; Zhao, X.; Addy, M. Design of a Control System for a Mini-Automatic Transplanting Machine of Plug Seedling. *Comput. Electron. Agric.* **2020**, *169*, 105226. [CrossRef]
35. Vlahidis, V.; Rosca, R.; Carlescu, P.-M. Evaluation of the Functional Parameters for a Single-Row Seedling Transplanter Prototype. *Agriculture* **2024**, *14*, 388. [CrossRef]

Disclaimer/Publisher's Note: The statements, opinions and data contained in all publications are solely those of the individual author(s) and contributor(s) and not of MDPI and/or the editor(s). MDPI and/or the editor(s) disclaim responsibility for any injury to people or property resulting from any ideas, methods, instructions or products referred to in the content.